GOAT: A Global Transformer on Large-scale Graphs

Kezhi Kong [1] Jiuhai Chen [1] John Kirchenbauer [1] Renkun Ni [1] C. Bayan Bruss [2] Tom Goldstein [1]

Abstract

Graph transformers have been competitive on graph classification tasks, but they fail to outperform Graph Neural Networks (GNNs) on node classification, which is a common task performed on large-scale graphs for industrial applications. Meanwhile, existing GNN architectures are limited in their ability to perform equally well on both homophilious and heterophilious graphs as their inductive biases are generally tailored to only one setting. To address these issues, we propose GOAT, a scalable global graph transformer. In GOAT, each node conceptually attends to all the nodes in the graph and homophily/heterophily relationships can be learnt adaptively from the data. We provide theoretical justification for our approximate global self-attention scheme, and show it to be scalable to large-scale graphs. We demonstrate the competitiveness of GOAT on both heterophilious and homophilious graphs with millions of nodes. We open source our implementation at https://github.com/devnkong/GOAT.

1. Introduction

Transformers (Vaswani et al., 2017) have demonstrated efficacy in many domains including language understanding and computer vision (Devlin et al., 2018; Dosovitskiy et al., 2020), and this has spurred interest in applying transformers to the graph domain. However, the success of transformers for graphs has been more modest, and has mostly been in the fairly narrow regime of graph classification tasks like molecule classification (Ying et al., 2021; Mialon et al., 2021; Hussain et al., 2021; Dwivedi & Bresson, 2020; Rong et al., 2020; Kreuzer et al., 2021; Maziarka et al., 2021). The success of transformers in this regime is largely a result of the small size of each problem instance. For instance, the mean node count of graphs from the `ogbg-molhiv` dataset of the *Open Graph Benchmark* (Hu et al., 2020a) is only 25.5. This tiny size enables self-attention across a larger percent of the graph, enabling *long-range* or even *global* self-attention. Despite a recent surge in interest in attention-based networks, standard Graph Neural Networks (GNNs) (Kipf & Welling, 2016; Veličković et al., 2017) are still the de-facto model of choice for broader applications involving node classification or large industrial graphs.

[1]University of Maryland, College Park [2]Capital One. Correspondence to: Kezhi Kong <kong@cs.umd.edu>, Tom Goldstein <tomg@cs.umd.edu>.

Proceedings of the 40^{th} International Conference on Machine Learning, Honolulu, Hawaii, USA. PMLR 202, 2023. Copyright 2023 by the author(s).

Research in other domains suggests that a transformer's ability to utilize long-range signals that were previously inaccessible in more constrained sequential models are its key success factor. However, it is well-known that this self-attention is expensive, with time and memory overhead growing quadratically with the length of the input. To address this issue for language transformers, a range of efficient variants have been proposed (Wang et al., 2020; Kitaev et al., 2020; Zaheer et al., 2020; Zhu et al., 2021; Choromanski et al., 2020) and have demonstrated competitive performance.

When applying transformers to graphs, sequence length is akin to the size l of the l-hop neighborhood, but the size grows exponentially instead of linearly. For large enough l, the model becomes *global* and attends to the entire graph. Tasks such as node classification are usually done on large-scale graphs such as `ogbn-products` (2.4M nodes). Attending to the entirety of this graph in a naive way would require 24TB of GPU memory (Geisler et al., 2021). It is an open and pressing challenge to design efficient graph transformer models that scale to graphs of this size. Existing works on graph transformers for node classification never go beyond recursive 1-*hop-neighbor* message passing (Shi et al., 2020; Zhao et al., 2021; Hu et al., 2020b) so they fail to learn from larger context and perhaps fail to achieve the full potential demonstrated in other domains.

At the same time, an established limitation of GNNs is their over-reliance on the homophily principle (McPherson et al., 2001) causing them to perform poorly on heterophilious graphs. Homophily (or heterophily) means that a node's neighbors are likely (unlikely) to be of the same class. Standard GNNs are built on the message passing scheme (Gilmer et al., 2017), where features are aggregated recursively between 1-hop neighbors. This scheme has strong inductive bias towards homophilious graphs and does not tolerate heterophily well. To address this, researchers have proposed various heterophily-centered GNN models (Lim et al., 2021; Abu-El-Haija et al., 2019; Pei et al., 2020; Zhu et al., 2020). These models usually involve specialized message passing schemes that do not work for homophilious graphs. GPR-GNN (Chien et al., 2020) can adapt to different homophily/heterophily profiles, but this model uses the entire graph for each training update ("full-batch" training) and thus cannot scale to huge problems. While it is reasonable to have specialized model designs for different kinds of graphs, this practice can be problematic when the homophily or heterophily characteristics of the target dataset are unknown, or the graph has mixed behavior.

Present work. We study a global transformer in which each node attends to all others, providing a universal architecture that supports both homophilious and heterophilious graphs. We propose GOAT, a global transformer for large-scale node classification tasks. To implement the intractable $O(n^2)$ global self-attention on large-scale graphs, we leverage a dimensionality reduction algorithm and reduce memory complexity from quadratic to linear. Using a K-Means based projection algorithm, we theoretically show that our scalable global attention method has bounded error relative to graph attention without dimensionality reduction. Besides the global design, we also strengthen the model using a scalable local attention module. For each node, we sample its l-hop neighbors and make it *directly* attend to them, unlike the recursive smoothing pattern of GNNs. Empirically, GOAT shows strong performance on both homophilious and heterophilious datasets as large as `ogbn-products` (2.4M nodes) (Hu et al., 2020a) and `snap-patents` (2.9M nodes) (Lim et al., 2021). We summarize our contributions as follows:

1. We propose GOAT, a scalable global transformer model where each node is able to attend to all others.
2. We develop a novel local attention module that enables GOAT to absorb rich local information.
3. We demonstrate the strong performance of GOAT on both large-scale homophilous and heterophilious node classification benchmarks.
4. We provide theoretical justification to show our scalable global attention scheme has bounded error relative to unscalable standard attention.

2. Preliminaries

In this section we introduce the preliminaries of GNNs, transformers, and homophily.

Graph Neural Networks (GNNs). We represent a graph as $\mathcal{G}(\mathcal{V}, \mathcal{E})$. GNNs are often built with recursive message-passing schemes, where features are passed and shared directly between 1-hop neighbors. Formally the k-th iteration of message passing, or the forward propogation of the k-th layer of GNNs, is defined as follows:

$$\begin{aligned} m_v^{(k)} &= \text{AGGREGATE}^{(k)}\left(\left\{\left(h_v^{(k-1)}, h_u^{(k-1)}, e_{uv}\right), \forall u \in \mathcal{N}(v)\right\}\right), \\ h_v^{(k)} &= \text{COMBINE}^{(k)}\left(h_v^{(k-1)}, m_v^{(k)}\right), \end{aligned} \quad (1)$$

where $h_v^{(k)}$ is the hidden feature of node v at the k-th layer, $m_v^{(k)}$ is the computed message for node v at the k-th layer, e_{uv} is the edge feature between node u and v, $\mathcal{N}(v)$ is node v's 1-hop neighbor set. AGGREGATE$(\cdot)$ and COMBINE$(\cdot)$ are functions parameterized by neural networks.

Transformers. The key component of a transformer model is the self-attention scheme, which allows each element of a set or token to attend to information of other tokens at various locations. The forward pass of a self-attention module is defined as:

$$\text{Attn}(H) = \text{Softmax}\left(\frac{HW_Q\left(HW_K\right)^\top}{\sqrt{d}}\right)HW_V, \quad (2)$$

where $H \in \mathbb{R}^{n\times f}$ is the hidden feature matrix. $W_Q, W_K, W_V \in \mathbb{R}^{f\times d}$ are linear projection matrices with trainable weights. Here the Equation 2 denotes the single-head self-attention module, which can straightforwardly generalize to multi-head attention. Note that in practice multi-headed self-attention is widely used. It is easy to see that attention is expensive. The time and memory complexity is $O(n^2)$, which leads to low efficiency and is a bottleneck for transformers. In this work, we call the output of the Softmax function the "attention matrix".

Homophily indicates connected nodes are likely to share common labels. We follow Lim et al. (2021) to focus on edge homophily in this work. The edge homophily is defined as the proportion of edges that link two nodes with the same label as below:

$$h = \frac{|\{(u, v) \in \mathcal{E} : y_u = y_v\}|}{|\mathcal{E}|}, \quad (3)$$

where $\mathcal{E}$ is the edge set and y is the node label. Non-homophily (or **heterophily**) graph indicates the dataset with dissimilar labels/features sharing edges.

3. Method

Intuition. Existing GNNs usually have hardcoded message-passing patterns and will only work on either homophilious or heterophilious graphs. A global attention scheme makes each node attend to all the nodes in the graph and does not explicitly have inductive bias towards either one. Instead of one specially tailored or fixed message passing and aggregating pattern, the attention scheme freely learns to adapt to different priors. Furthermore, the ability to attend to a single far-away node may enable multi-hop features to be used without the over-smoothing that happens when information is passed over many rounds of averaging in a standard GNN. However, for applications in industry where large graphs with millions of nodes are ubiquitous, it is not possible to train and deploy a fully global transformer due to the quadratic cost.

Given that, we propose **GOAT**, the scalable $\underline{\text{g}}$l$\underline{\text{o}}$b$\underline{\text{a}}$l $\underline{\text{t}}$ransformer. GOAT uses an approximate global attention which reduces complexity from quadratic to linear and supports mini-batch training. GOAT also has a local attention module to process information from the local neighborhood for better prediction. Figure 1 illustrates the local sampling procedure and the whole attention module. In this section, we describe our methodological designs in detail. Firstly let us have a formal definition on the notations.

Definition 3.1. We define n as the total number of nodes in the graph, k is the number of dimension in the low dimensional space, $k \ll n$. P denotes the projection matrix, $P \in \mathbb{R}^{n\times k}$. f denotes the raw feature dimension of the node feature and d is the hidden feature dimension if without further specification. b denotes batch size.

Global. To address the expensive quadratic complexity issue, we leverage *dimensionality reduction*. Firstly we want to find a projection matrix P that can reduce the feature matrices into a low-dimensional space so the cost of computing their product is reduced. At the same time we also hope this reduction will not overly degrade the quality of representations. Below, we provide theoretical analysis on the existence of such matrix, P. Note that in the demonstration process below, we assume positional information is already fused into node features.

Theorem 3.2. *For any linear weight matrices $W_K, W_Q, W_V \in \mathbb{R}^{f\times d}$, node feature matrix $X \in \mathbb{R}^{n\times f}$, mini-batch of nodes $X_B \in \mathbb{R}^{b\times f}$, row vector $x \in \mathbb{R}^{1\times n}$ of X, and $\varepsilon > 0$, there exists projection matrices $P_A, P_V \in \mathbb{R}^{n\times k}$, such that*

$$\Pr(\left\|\text{Softmax}\left(SP_A\right)P_V^\top XW_V - \text{Softmax}(S)XW_V\right\|_F \leqslant \varepsilon \|\text{Softmax}(S)\|_F\,\|XW_V\|_F) > 1 - O(1/n), \quad (4)$$

with $S = X_B W_Q \left(XW_K\right)^\top / \sqrt{d}$ and $k = O\left(\log(n)/\varepsilon^2\right)$.

We argue that the scheme provided by Theorem 3.2 makes global attention possible on large graphs. The expression $SP_A = \left(X_B W_Q \left(XW_K\right)^\top / \sqrt{d}\right) P_A$ inside the Softmax function can be computed as a product between $Q_B = X_B W_Q$ and $\widetilde{K} = P_A^\top XW_K$, which is only $O(bdk)$ work. Note that the new value feature matrix $\widetilde{V} = P_V^\top XW_V$ is also low dimensional. Then we see that the problem comes to how we can materialize $\widetilde{K}, \widetilde{V}$ without explicitly computing the multiplication of $(XW_K)^\top P_A$ or $P_V^\top XW_V$ which is $O(nfd + nkd)$ and not scalable when the graph is large.

Technically, we follow Van Den Oord et al. (2017) to materialize $\widetilde{K}$ and $\widetilde{V}$. Projection matrix P is computed by the K-Means algorithm as the sparse indexing matrix. Each row of $P \in \mathbb{R}^{n\times k}$ is a one-hot vector representing the clustering centroid the node is assigned to. We define

$$C = \text{diag}^{-1}(\mathbf{1}_n P)P^\top X$$

as the *codebook*. Each row of the codebook C represents the center (e.g., the average) of all the entries in a cluster. In this way, $\widetilde{K} = \text{diag}^{-1}(\mathbf{1}_n P)P^\top XW_K = CW_K$ and $\widetilde{V} = \text{diag}^{-1}(\mathbf{1}_n P)P^\top XW_V = CW_V$. We store and update $\widetilde{K}, \widetilde{V}$ in the exponential moving average (EMA) manner. The algorithm is summmarized in Algorithm 2. Note that we do not explicitly compute $\widetilde{K}, \widetilde{V}$ each iteration but instead cache and update the codebook on the fly in the EMA manner using batch statistics. P is stored sparsely to save memory.

Now we go back to show that the forward pass under such a scheme yields a bounded-error approximation compared with the authentic output. We start with two definitions for clearer demonstration. We define

$$\widetilde{X} = P\text{diag}^{-1}(\mathbf{1}_n P)P^\top X = PC, \quad (5)$$

as the approximate X using the codebook. We define the attention matrix for a batch X_B computed by parameterized function f_W as

$$f_W(Y) = \text{Softmax}\left(\frac{X_B W_Q\left(YW_K\right)^\top}{\sqrt{d}}\right). \quad (6)$$

Theorem 3.3. *If the function f_W has Lipschitz constant upper-bounded by* lip (f_W) *and the quantization error is ε, the estimation error is bounded as,*

$$\left\|\widetilde{X}_B^{out} - X_B^{out}\right\|_F \leq \varepsilon\cdot[1 + O\left(\text{lip}\left(f_W\right)\right)]\,\|A_B\|_F\cdot\|X\|_F\cdot\|W_V\|_F\,, \quad (7)$$

with $\widetilde{X}_B^{out} = \widetilde{A}_B\widetilde{X}W_V$, $X_B^{out} = A_B XW_V$, $A_B = f_W(X) = \text{Softmax}\left(X_B W_Q\left(XW_K\right)^\top/\sqrt{d}\right)$, and $\widetilde{A}_B = f_W(\widetilde{X}) = \text{Softmax}\left(X_B W_Q(\widetilde{X}W_K)^\top/\sqrt{d}\right)$. Quantization error ε is defined as $\|X - \widetilde{X}\|_F \leq \varepsilon\|X\|_F$.

Note that the computation of $\widetilde{X}_B^{\text{out}}$ denoted in Theorem 3.3, which is the approximated global attention, is expensive because it requires the computation of matrix multiplication

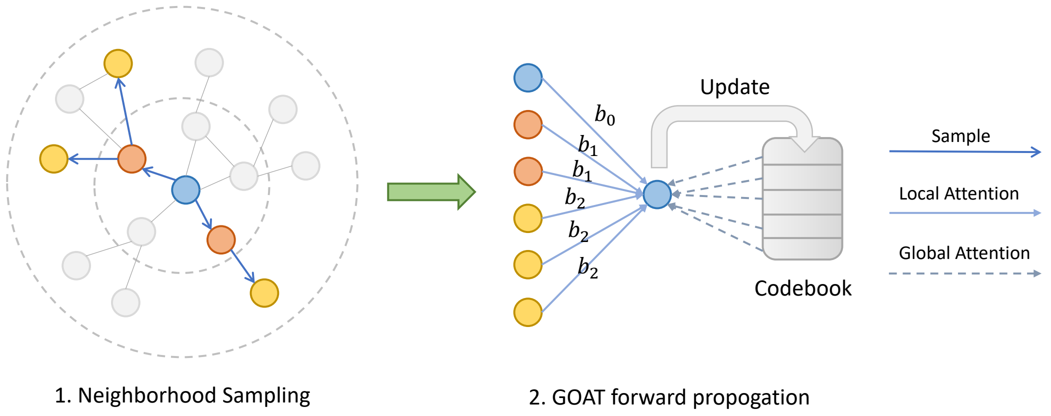

Figure 1: The local sampling procedure and forward propogation of the GOAT model. b_l denotes the trainable positional bias for neighbors at a distance of l.

Algorithm 1 Global Transformer mini-batch forward propogation algorithm

```
Require: Graph $\mathcal{G} = (\mathcal{V}, \mathcal{E})$; $\mathrm{MLP}_\mathrm{a}$ and $\mathrm{MLP}_\mathrm{b}$ are two independent MLPs; PE is the precomputed positional encoding based on the structure of graph $\mathcal{G}$; $\mu_x, \mu_{pe}$ are the centroids computed by the K-Means algorithm; $P$ is the centroid assignment index for each node; $W_Q, W_K, W_V$ are trainable parameters.
for $v \in \mathcal{V}$ do
    $x \leftarrow \mathrm{MLP}_\mathrm{a}(X_v)$
    $pe \leftarrow PE_v$
    $q \leftarrow \mathrm{Concat}(x, pe)W_Q$
    $K \leftarrow \mathrm{Concat}(\mu_x, \mu_{pe})W_K$
    $V \leftarrow \mu_x W_V$
    $x_{out} \leftarrow \mathrm{Softmax}\left(\frac{qK^\top}{\sqrt{d}} + \log(\mathbf{1}_n P)\right) V$
    $x_{out} \leftarrow \mathrm{MLP}_\mathrm{b}(x_{out})$
    Update $\mu_x, \mu_{pe}$ by $x, pe$ using the EMA K-Means algorithm as in Algorithm 2.
end for
```

of $X_B W_Q \widetilde{X} W_K$ and also $\widetilde{A}_B \widetilde{X} W_V$, which is unscalable. We articulate it in this way for the simplicity of theoretical proof. Below we show that $\widetilde{X}_B^{\text{out}}$ can be equivalently computed using $\widetilde{K}$ and $\widetilde{V}$, which are low-dimensional.

Corollary 3.4. *The computation of* $\widetilde{X}_B^{out} = \mathrm{Softmax}\left(X_B W_Q (\widetilde{X} W_K)^\top / \sqrt{d}\right) \widetilde{X} W_V$ *is equivalent with*

$$\widetilde{X}_B^{out} = \mathrm{Softmax}\left(X_B W_Q \widetilde{K}^\top / \sqrt{d} + \log(\mathbf{1}_n P)\right) \widetilde{V}. \quad (8)$$

All the proofs are deferred to the Appendix.

Through Corollary 3.4, where X_B gets to directly attends to $\widetilde{K} = C W_K$ instead of $\widetilde{X}$. As we have discussed, both $\widetilde{K}$ and $\widetilde{V}$ will be materialized in memory and updated in the EMA way. The computation for the feature of a node $\widetilde{X}_B^{\text{out}}$ is $O(bdk)$ and thus scalable and efficient. Algorithm 1 illustrates our global transformer forward pass.

Algorithm 2 EMA K-Means update algorithm

```
Require: Inputs are the hidden features $X$ and positional encodings $PE$ for a batch. $\mathrm{bn}(\cdot)$ is the batch norm module. $\mathrm{FindNearest}(\cdot)$ finds the nearest centroid for each feature.
function Update($X, PE$)
    $F \leftarrow \mathrm{Concat}(X, PE)$
    $F \leftarrow \mathrm{bn}(F)$ {data whitening using batch norm}
    $\mu \leftarrow \mathrm{Concat}(\mu_x, \mu_{pe})$
    $P \leftarrow \mathrm{FindNearest}(F, \mu)$ {compute cluster assignment}
    $c \leftarrow c \cdot \gamma + P^\top \mathbf{1} \cdot (1 - \gamma)$ {EMA accumulation}
    $v \leftarrow v \cdot \gamma + P^\top F \cdot (1 - \gamma)$ {EMA accumulation}
    $v \leftarrow v / c$
    $\mu \leftarrow v \cdot \mathrm{bn.running\_std} + \mathrm{bn.running\_mean}$
    $\mu_x, \mu_{pe} \leftarrow \mu$
end function
```

It is well established in the literature that good positional encodings are required to make transformers work effectively. In our global attention scheme, only absolute positional encodings are feasible because the hidden features and positional encodings must be concatenated. We argue that the design of positional encoding on graphs is still an open question for the community (Dwivedi et al., 2021; Kreuzer et al., 2021) and detailed discussion for such design is beyond the scope of this work. To simplify the setup of the experiments, we use pretrained node2vec (Grover & Leskovec, 2016) node embeddings as our positional embeddings.

Local. Along with the design of our global transformer, we propose a novel local attention module, which allows each node to *directly* attend to its l-hop neighbors to attain rich local information. Empirically, we find that the local attention module effectively helps the model learn better representations. Although this module is responsible for aggregating information from the *local* neighborhood as in normal message passing feature aggregation, unlike the standard GNNs' recursive 1-hop neighbor smoothing pattern, our local module provides flexible attention weights for neighbors at different hop distances. We believe the module provides increased capacity to learn the inductive biases required for accurate predictions beyond the hard-coded structures of existing GNNs. To support mini-batch training, we adopt the widely-used neighbor sampling (NS) method (Hamilton et al., 2017) to sample all l-hop neighbors. We make each node directly attend to the sampled neighbors. Inspired by Ying et al. (2021), for the local module we select the *relative* positional encoding scheme to distinguish neighbors at diverse distances from the source node. Our attention score calculation inside the Softmax function is:

$$S_{ij} = \frac{X_i W_Q \left(X_j W_K\right)^\top}{\sqrt{d}} + b_{D(i,j)}, \tag{9}$$

where $b_{D(i,j)}$ is a trainable bias parameter indexed by $D(i,j)$, the shortest distance between node i and j. Note that although the local module intuitively helps learn better representations, the neighbor sampling (NS) algorithm does introduce a small scalability concern. It is well-known that the neighborhood explosion problem for NS has complexity $O(d^l)$ for l-hop neighborhoods, where d is the average degree of the graph. Surprisingly, it is the NS step, and not the approximate global attention, that is the primary efficiency bottleneck for our model. We investigate the efficiency perspective in Section 5.

Since we leverage different positional encodings for the global and local modules, we have separate attention functions, after which the respective sets of node features and positional encodings are concatenated and fed into subsequent layers. Figure 1 illustrates the local sampling procedure and the whole attention module. In the sections to follow, we show that GOAT displays strong performance on the large-scale node classification task.

4. Experiments

In this section, we detail the empirical evaluation of our GOAT model.

Datasets. We select four datasets to evaluate. To represent homophilious graph problems we choose two datasets, `ogbn-arxiv` and `ogbn-products`, from the well-known *Open Graph Benchmark* (OGB) (Hu et al., 2020a). For heterophilious examples we utilize the `arxiv-year` and `snap-patents` datasets curated by Lim et al. (2021). These are all large-scale (multi-million) node classification datasets. For the train and validation splits, we use the official splits from OGB for both `ogbn-arxiv` and `ogbn-products` and for `arxiv-year` and `snap-patents` we follow the practice of Lim et al. (2021) and randomly sample the train and validation sets. As there are no official splits or train set ratios for these two datasets, we experiment with training sets that comprise 10%, 20%, and 50% of the data while fixing validation set ratio at 25%, and report separate results for each split. We refer readers to Table 1 for detailed statistics of the datasets.

Setup. We focus on the transductive node classification task, where we see all the nodes at training time, but only the train set has labels. Our baseline models include GCNJK (Xu et al., 2018), GAT (Veličković et al., 2017), LINKX (Lim et al., 2021), MixHop (Abu-El-Haija et al., 2019), and GPS (Rampášek et al., 2022). All of our training procedures use pure empirical risk minimization (ERM) and we do not leverage techniques like data augmentation (Kong et al., 2020), label propogation (Huang et al., 2020), powerful embeddings (Chien et al., 2021), or other tricks, as these additional regularizers have not been uniformly studied for all model types, and this simple setting enables fair comparisons across model architectures. For the baseline models, we perform a hyperparameter sweep and select the best performing settings and report the corresponding results for each model and dataset pairing (full details in the Appendix). For GOAT, the attention function is multi-headed but we only implement a single layer of attention module. We leave the discussion of a multi-layer variant to future work. For the local attention, we sample neighbors that live within 3-hops. For each node we sample [20, 10, 5] neighbors recursively. The size of the codebook is fixed at $4,096$ and the dimensionality is 64. We always use a dropout rate of 0.5 and also use batch norm. Each experiment is carried out on either a single GeForce RTX 2080 Ti (11GB memory) or a RTX A4000 (16GB memory).

Results. Table 2 reveals the competitive performance of our GOAT model compared with baselines. For * we show performance of MixHop with GraphSAINT sampling (Zeng et al., 2019) on `snap-patents` despite Lim et al. (2021) reporting 46.82 ± 0.11 for MixHop with ClusterGCN sampling (Chiang et al., 2019) as their runner-up to LINKX on this dataset. This setting was OOM/T on our hardware, but as it is weaker than LINKX and GOAT in either case, reporting the stronger numbers would not have changed the results or analysis of average model performance. GCNJK and GAT intuitively register strong performances on `ogbn-arxiv` and `ogbn-products` as they resonate with the inductive bias of the two homophilious datasets. In contrast, on the `arxiv-year` and `snap-patents` datasets, their scores are poor. LINKX and MixHop are architectures designed for heterophilious graphs, a specialization validated by their strong performances in Table 2 on those datasets. However, GOAT constantly achieves competitive results on *all four* datasets, which reveals the adaptive ability of the attention functions. We highlight that our goal is not to beat GNNs universally; specific priors can still be useful factors when designing architectures. Further, in accordance with the no-free-lunch theorem, winning

Table 1: Dataset statistics.

Dataset	# Nodes	# Edges	# Feat.	# Class	Class type	Split	Edge hom.
ogbn-arxiv	169,343	1,166,243	128	40	product category	official	.66
ogbn-products	2,449,029	61,859,140	100	47	subject area	official	.81
arxiv-year	169,343	1,166,243	128	5	pub year	random	.222
snap-patents	2,923,922	13,975,788	269	5	time granted	random	.073

all comparisons on datasets with diverse properties is expected to be difficult. Rather, our intention is to develop a model that can learn different inductive biases as required, adapting seamlessly to different use cases. This flexibility is an important quality in practice as practitioners may encounter datasets for which knowledge about appropriate priors is scarce. Note that we further try to compare with GPS (Rampášek et al., 2022), which is a powerful scalable graph transformer on graph-level tasks. However on large-scale node tasks GPS always yields OOM even on the smallest arxiv datasets.

5. Ablation Studies & Analysis

GOAT vs. GOAT-Local-only. In Figure 2a & 2b we ablate to only use the local module to analyze our architecture design. On the ogbn-arxiv dataset where homophily is prevalent, the local-only model is as strong as the complete GOAT. While on the arxiv-year dataset there shows clear discrepancy between the two, where the global module brings a salient 3% boost. The results provide a strong validatioin towards our main intuition, that the global module increases expressive power by modeling long-range interactions. And such ability is especially effective towards heterophilious graphs, which is intuitive as many other successful heterophilious GNN architectures aimed at broadening the range of message passing as well as learning from long-range interactions.

Codebook size. We run ablation studies on the codebook size for a better understanding and interpretation of the GOAT model. The codebook size refers to the k value in the K-Means algorithm. We summarize the results in Table 3. Note the heterophilious dataset arxiv-year is more sensitive to the adjustment of the codebook size, showing the efficacy of global attention module at learning long-range interactions.

Batch norm vs. Layer norm. Normalization is important to transformers. We ablate on the normalization technique selection in Figure 3a & 3b. We see that layer norm can be as good as batch norm in our model but converges much slower, and evidently "no normalization" is not a good choice for our architecture.

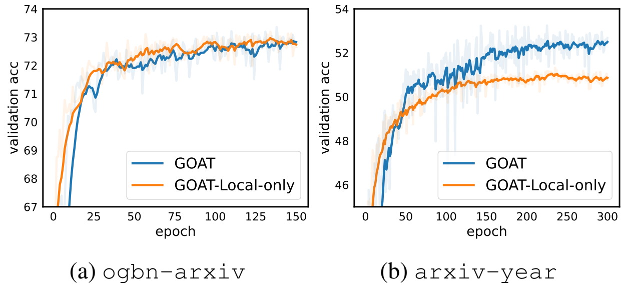

(a) ogbn-arxiv (b) arxiv-year

Figure 2: Ablation study on the local module.

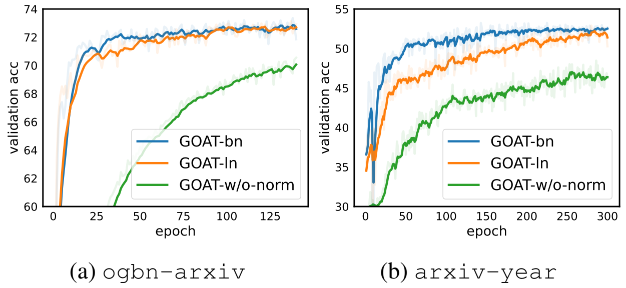

(a) ogbn-arxiv (b) arxiv-year

Figure 3: Ablation study on the normalization technique.

Depth. We constantly have 1 layer of attention modules in our model, for both the global and local part. In fact it is challenging to extend our GOAT model to multi-layer attention computation like common transformers. Note that our attention modules are not strict *self-attention* modules, whose input and output are of the same length. As denoted in Fig 1, our input includes the predictive node, sampled neighbors, and the codebook, but only the the predictive node attends to others and gets aggregated features. So after the attention function the state of feature for sampled neighbors and the codebook is behind that of the predictive node, where future rounds of attention computation is less intuitive. A straightforward strategy to address this conundrum is to recursively sample neighbors of neighbors and add more codebooks by each layer, but apparently this will greatly adds to the overhead and renders the model less efficient. Due to computational limitation we do not carry out the experiments, but how to make the model deeper is

Table 2: Experimental results. Note that the "Overall performance average" is the mean value of the two "Performance avgerage" values in the upper and lower tables. The darker blue marks the best result in each row, while the lighter shade marks the runner-up. Evaluation metric is prediction accuracy on the test set. Test accuracies are reported based on the hyperparameter setting yielding the highest validation accuracies. Where possible, we validate our baselines against the results in Lim et al. (2021). OOM means out of memory error through our experiments.

		General GNN		Heterophilious GNN		Transformer	Ours
Dataset	Train ratio	GCNJK	GAT	LINKX	MixHop	GPS	GOAT
`ogbn-arxiv`	official 54%	69.57 ± 0.20	71.95 ± 0.36	66.18 ± 0.33	71.29 ± 0.29	OOM	72.41 ± 0.40
`ogbn-products`	official 8%	72.84 ± 0.36	79.45 ± 0.59	71.59 ± 0.71	73.48 ± 0.29	OOM	82.00 ± 0.43
Performance average		71	76	69	72	OOM	77
`arxiv-year`	random 10%	43.34 ± 0.08	38.34 ± 0.10	46.22 ± 0.24	45.13 ± 0.25	OOM	49.44 ± 0.11
`arxiv-year`	random 20%	44.77 ± 0.10	39.19 ± 0.12	49.16 ± 0.42	47.18 ± 0.24	OOM	51.21 ± 0.44
`arxiv-year`	random 50%	47.74 ± 0.23	40.27 ± 0.20	53.53 ± 0.36	50.37 ± 0.25	OOM	53.57 ± 0.18
`snap-patents`	random 10%	32.50 ± 0.10	32.72 ± 0.10	49.74 ± 0.46	33.57 ± 0.06	OOM	44.31 ± 0.43
`snap-patents`	random 20%	32.97 ± 0.06	32.96 ± 0.09	54.32 ± 0.50	33.96 ± 0.06	OOM	49.55 ± 0.31
`snap-patents`	random 50%	33.52 ± 0.05	33.10 ± 0.09	60.12 ± 0.23	34.28 ± 0.07*	OOM	54.97 ± 0.23
Performance average		39	36	52	41	OOM	51
Overall performance average		55	56	61	57	OOM	64

Table 3: Codebook size abalation study.

codebook size	`ogbn-arxiv`	`arxiv-year`
512	71.92	50.90
$1k$	71.99	51.21
$2k$	72.14	52.51
$4k$	72.41	53.57

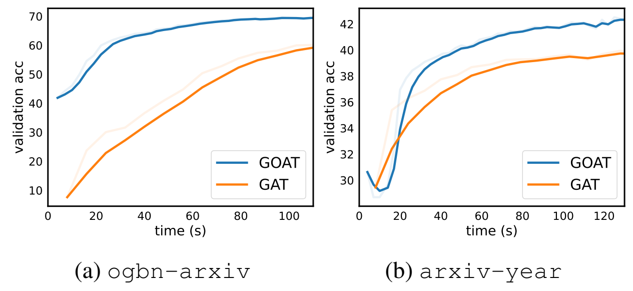

Figure 4: Convergence speed comparison.

an interesting research opportunity.

Efficiency. The neighbor sampling bottleneck is the major limitation of our method. Note that although the local module intuitively helps learn better representations, the neighbor sampling (NS) algorithm does introduce a small scalability concern. It is well-known that the neighborhood explosion problem for NS has complexity $O(d^l)$ for l-hop neighborhoods, where d is the average degree. Our sampling method in the local module is a plain adaptation of NS so that GOAT will share efficiency issues of NS. However when we only use the global module of GOAT, its convergence rate outperforms that of GAT-NS by a large margin according to Figure 4a and Figure 4b due to the linear complexity benefit. In Table 4 we report the absolute elapsed running time per training epoch for GAT-NS and GOAT on datasets with $1k$ and $4k$ as batch size. We see that GOAT has competitive running speed compared with GAT that is powered by NS for scalable training, while our GOAT-Global-only variant overwhelmingly outperforms the other two thanks to the linear training complexity. Detailed hyperparameter setup can be found in the Appendix.

6. Related Work

Scalability. The poor scalability of GNNs to large graphs remains a major obstacle to deploying GNNs for enterprise-scale applications. Scalable GNN algorithms mainly involve node-, layer-, and graph-wise sampling methods.

Table 4: Running time in second (s) per epoch of different models. GOAT-G refers to GOAT-Global-only model variant.

batch size	model	ogbn-arxiv	ogbn-products
1k	GAT	9.76	127.42
1k	GOAT-G	2.88	5.58
1k	GOAT	8.00	109.51
4k	GAT	8.31	113.47
4k	GOAT-G	2.33	4.36
4k	GOAT	7.62	101.73

Hamilton et al. (2017) proposed neighbor sampling (NS) to repeatedly sample neighbors for message passing, but this approach leads to the exponential neighborhood explosion problem mentioned at the end of Section 3. One technique to address this issue is the layer-wise sampling proposed in Huang et al. (2018). ClusterGCN (Chiang et al., 2019) and GraphSAINT (Zeng et al., 2019) both perform subgraph sampling so that GNNs can be run in a "full-batch" manner but on tractable subgraphs that hopefully approximate the global graph semantics - we employ the latter of the two for training our baseline GCNJK, GAT, and MixHop models. A recent method, GAS (Fey et al., 2021), stores historical node features to help both training and inference process. Finally, it is also established that transformers suffer from inherent scalability issues. In response, a plethora of efficient transformers have been proposed that employ different techniques to improve their complexity including sparse attention maps (Zaheer et al., 2020; Beltagy et al., 2020), clustering-based schemes (Kitaev et al., 2020; Tay et al., 2020), and low-rank projections of the attention matrix (Wang et al., 2020; Tay et al., 2021).

Graph transformers. Most successful applications of transformers to graphs problems have only considered graph classification. Graphormer (Ying et al., 2021) is the representative global transformer on small graphs with customized centrality, edge, and spatial encodings. Other strong architectures include Kreuzer et al. (2021); Maziarka et al. (2021); Dwivedi & Bresson (2020); Rong et al. (2020). Existing graph transformers (Shi et al., 2020; Hu et al., 2020b; Dwivedi & Bresson, 2020; Rampášek et al., 2022) for node classification use the same recursive message passing scheme as traditional GNNs. The attention module computes attention scores as the weights for 1-hop neighborhood smoothing, similar to the attention mechanism in GATs (Veličković et al., 2017). These models fail to demonstrate the ability to learn from larger contexts and generally do not outperform traditional GNNs. An example architecture that does implement a form of global attention, GraphBERT (Zhang et al., 2020), fails to solve scalabilty issues due to requiring full-batch training.

Heterophily. Recently a body of work has focused on adapting GNNs to heterophilious graphs. LINKX (Lim et al., 2021) is a simple model that coerces 2-hop (but not 1-hop) neighbors to have the similar labels. H2GCN (Zhu et al., 2020) aggregates features from 1-hop and 2-hop neighbors separately. MixHop (Abu-El-Haija et al., 2019) aggregates information from diverse degrees of smoothed features. GPR-GNN (Chien et al., 2020) is similar to MixHop, but uses a more complex adaptive aggregation operation. GPR-GNN works well on some kinds of data but does not scale to large graphs. One closely related work is Non-local GNN (Liu et al., 2021), which does an approximate global attention leveraging attention-based sorting. The model successfully reduces time complexity from $O(n^2)$ to $O(nlog(n))$, but cannot support mini-batch training, so its scalability is limited.

While progress has certainly been made towards more effective graph transformers and models specifically suited to heterophilious graphs, to date, no graph transformer has emerged that simultaneously relaxes the restriction of a homophilious inductive bias (whilst remaining performant in that setting) and easily handles large-scale node classification tasks.

7. Conclusion

We propose GOAT, a global transformer that works on both homophilious and heterophilious node classification tasks. Our model makes global attention possible by dimensionality reduction and we prove our approximate approach has bounded error compared with the true global mechanism. Experiments reveal GOAT's strong performances on large-scale graphs. We hope our work can spur more research into universal graph neural architecture who can adapt to different inductive biases.

Acknowledgements

This work was made possible by support from Capital One Bank and the National Science Foundation (IIS-2212182), the ONR MURI program, DARPA GARD (HR00112020007), the Office of Naval Research (N000142112557), and the AFOSR MURI program. Commercial support was provided by Capital One Bank, the Amazon Research Award program, and Open Philanthropy. Further support was provided by the National Science Foundation (IIS-2212182), and by the NSF TRAILS Institute (2229885).

References

Abu-El-Haija, S., Perozzi, B., Kapoor, A., Alipourfard, N., Lerman, K., Harutyunyan, H., Ver Steeg, G., and Galstyan, A. Mixhop: Higher-order graph convolutional architectures via sparsified neighborhood mixing. In *international conference on machine learning*, pp. 21–29. PMLR, 2019.

Beltagy, I., Peters, M. E., and Cohan, A. Longformer: The long-document transformer. *arXiv preprint arXiv:2004.05150*, 2020.

Chiang, W.-L., Liu, X., Si, S., Li, Y., Bengio, S., and Hsieh, C.-J. Cluster-gcn: An efficient algorithm for training deep and large graph convolutional networks. In *Proceedings of the 25th ACM SIGKDD International Conference on Knowledge Discovery & Data Mining*, pp. 257–266, 2019.

Chien, E., Peng, J., Li, P., and Milenkovic, O. Adaptive universal generalized pagerank graph neural network. *arXiv preprint arXiv:2006.07988*, 2020.

Chien, E., Chang, W.-C., Hsieh, C.-J., Yu, H.-F., Zhang, J., Milenkovic, O., and Dhillon, I. S. Node feature extraction by self-supervised multi-scale neighborhood prediction. *arXiv preprint arXiv:2111.00064*, 2021.

Choromanski, K., Likhosherstov, V., Dohan, D., Song, X., Gane, A., Sarlos, T., Hawkins, P., Davis, J., Mohiuddin, A., Kaiser, L., et al. Rethinking attention with performers. *arXiv preprint arXiv:2009.14794*, 2020.

Devlin, J., Chang, M.-W., Lee, K., and Toutanova, K. Bert: Pre-training of deep bidirectional transformers for language understanding. *arXiv preprint arXiv:1810.04805*, 2018.

Dosovitskiy, A., Beyer, L., Kolesnikov, A., Weissenborn, D., Zhai, X., Unterthiner, T., Dehghani, M., Minderer, M., Heigold, G., Gelly, S., et al. An image is worth 16x16 words: Transformers for image recognition at scale. *arXiv preprint arXiv:2010.11929*, 2020.

Dwivedi, V. P. and Bresson, X. A generalization of transformer networks to graphs. *arXiv preprint arXiv:2012.09699*, 2020.

Dwivedi, V. P., Luu, A. T., Laurent, T., Bengio, Y., and Bresson, X. Graph neural networks with learnable structural and positional representations. *arXiv preprint arXiv:2110.07875*, 2021.

Fey, M., Lenssen, J. E., Weichert, F., and Leskovec, J. Gnnautoscale: Scalable and expressive graph neural networks via historical embeddings. In *International Conference on Machine Learning*, pp. 3294–3304. PMLR, 2021.

Geisler, S., Schmidt, T., Şirin, H., Zügner, D., Bojchevski, A., and Günnemann, S. Robustness of graph neural networks at scale. *Advances in Neural Information Processing Systems*, 34, 2021.

Gilmer, J., Schoenholz, S. S., Riley, P. F., Vinyals, O., and Dahl, G. E. Neural message passing for quantum chemistry. In *International conference on machine learning*, pp. 1263–1272. PMLR, 2017.

Grover, A. and Leskovec, J. node2vec: Scalable feature learning for networks. In *Proceedings of the 22nd ACM SIGKDD international conference on Knowledge discovery and data mining*, pp. 855–864, 2016.

Hamilton, W., Ying, Z., and Leskovec, J. Inductive representation learning on large graphs. *Advances in neural information processing systems*, 30, 2017.

Hu, W., Fey, M., Zitnik, M., Dong, Y., Ren, H., Liu, B., Catasta, M., and Leskovec, J. Open graph benchmark: Datasets for machine learning on graphs. *Advances in neural information processing systems*, 33:22118–22133, 2020a.

Hu, Z., Dong, Y., Wang, K., and Sun, Y. Heterogeneous graph transformer. In *Proceedings of The Web Conference 2020*, pp. 2704–2710, 2020b.

Huang, Q., He, H., Singh, A., Lim, S.-N., and Benson, A. R. Combining label propagation and simple models out-performs graph neural networks. *arXiv preprint arXiv:2010.13993*, 2020.

Huang, W., Zhang, T., Rong, Y., and Huang, J. Adaptive sampling towards fast graph representation learning. *Advances in neural information processing systems*, 31, 2018.

Hussain, M. S., Zaki, M. J., and Subramanian, D. Edge-augmented graph transformers: Global self-attention is enough for graphs. *arXiv preprint arXiv:2108.03348*, 2021.

Johnson, W. B. and Lindenstrauss, J. Extensions of lipschitz mappings into a hilbert space 26. *Contemporary mathematics*, 26:28, 1984.

Kane, D. M. and Nelson, J. Sparser johnson-lindenstrauss transforms. *Journal of the ACM (JACM)*, 61(1):1–23, 2014.

Kipf, T. N. and Welling, M. Semi-supervised classification with graph convolutional networks. *arXiv preprint arXiv:1609.02907*, 2016.

Kitaev, N., Kaiser, Ł., and Levskaya, A. Reformer: The efficient transformer. *arXiv preprint arXiv:2001.04451*, 2020.

Kong, K., Li, G., Ding, M., Wu, Z., Zhu, C., Ghanem, B., Taylor, G., and Goldstein, T. Flag: Adversarial data augmentation for graph neural networks. *arXiv preprint arXiv:2010.09891*, 2020.

Kreuzer, D., Beaini, D., Hamilton, W., Létourneau, V., and Tossou, P. Rethinking graph transformers with spectral attention. *Advances in Neural Information Processing Systems*, 34, 2021.

Lim, D., Hohne, F., Li, X., Huang, S. L., Gupta, V., Bhalerao, O., and Lim, S. N. Large scale learning on non-homophilous graphs: New benchmarks and strong simple methods. *Advances in Neural Information Processing Systems*, 34, 2021.

Liu, M., Wang, Z., and Ji, S. Non-local graph neural networks. *IEEE Transactions on Pattern Analysis and Machine Intelligence*, 2021.

Maziarka, L., Majchrowski, D., Danel, T., Gaiński, P., Tabor, J., Podolak, I., Morkisz, P., and Jastrzebski, S. Relative molecule self-attention transformer. *arXiv preprint arXiv:2110.05841*, 2021.

McPherson, M., Smith-Lovin, L., and Cook, J. M. Birds of a feather: Homophily in social networks. *Annual review of sociology*, 27(1):415–444, 2001.

Mialon, G., Chen, D., Selosse, M., and Mairal, J. Graphit: Encoding graph structure in transformers. *arXiv preprint arXiv:2106.05667*, 2021.

Pei, H., Wei, B., Chang, K. C.-C., Lei, Y., and Yang, B. Geom-gcn: Geometric graph convolutional networks. *arXiv preprint arXiv:2002.05287*, 2020.

Rampášek, L., Galkin, M., Dwivedi, V. P., Luu, A. T., Wolf, G., and Beaini, D. Recipe for a general, powerful, scalable graph transformer. *arXiv preprint arXiv:2205.12454*, 2022.

Rong, Y., Bian, Y., Xu, T., Xie, W., Wei, Y., Huang, W., and Huang, J. Self-supervised graph transformer on large-scale molecular data. *Advances in Neural Information Processing Systems*, 33:12559–12571, 2020.

Shi, Y., Huang, Z., Feng, S., Zhong, H., Wang, W., and Sun, Y. Masked label prediction: Unified message passing model for semi-supervised classification. *arXiv preprint arXiv:2009.03509*, 2020.

Tay, Y., Bahri, D., Yang, L., Metzler, D., and Juan, D.-C. Sparse sinkhorn attention. In *International Conference on Machine Learning*, pp. 9438–9447. PMLR, 2020.

Tay, Y., Bahri, D., Metzler, D., Juan, D.-C., Zhao, Z., and Zheng, C. Synthesizer: Rethinking self-attention for transformer models. In *International Conference on Machine Learning*, pp. 10183–10192. PMLR, 2021.

Van Den Oord, A., Vinyals, O., et al. Neural discrete representation learning. *Advances in neural information processing systems*, 30, 2017.

Vaswani, A., Shazeer, N., Parmar, N., Uszkoreit, J., Jones, L., Gomez, A. N., Kaiser, Ł., and Polosukhin, I. Attention is all you need. *Advances in neural information processing systems*, 30, 2017.

Veličković, P., Cucurull, G., Casanova, A., Romero, A., Lio, P., and Bengio, Y. Graph attention networks. *arXiv preprint arXiv:1710.10903*, 2017.

Wang, S., Li, B. Z., Khabsa, M., Fang, H., and Ma, H. Linformer: Self-attention with linear complexity. *arXiv preprint arXiv:2006.04768*, 2020.

Xu, K., Li, C., Tian, Y., Sonobe, T., Kawarabayashi, K.-i., and Jegelka, S. Representation learning on graphs with jumping knowledge networks. In Dy, J. and Krause, A. (eds.), *Proceedings of the 35th International Conference on Machine Learning*, volume 80 of *Proceedings of Machine Learning Research*, pp. 5453–5462. PMLR, 10–15 Jul 2018. URL https://proceedings.mlr.press/v80/xu18c.html.

Ying, C., Cai, T., Luo, S., Zheng, S., Ke, G., He, D., Shen, Y., and Liu, T.-Y. Do transformers really perform badly for graph representation? *Advances in Neural Information Processing Systems*, 34, 2021.

Zaheer, M., Guruganesh, G., Dubey, K. A., Ainslie, J., Alberti, C., Ontanon, S., Pham, P., Ravula, A., Wang, Q., Yang, L., et al. Big bird: Transformers for longer sequences. *Advances in Neural Information Processing Systems*, 33:17283–17297, 2020.

Zeng, H., Zhou, H., Srivastava, A., Kannan, R., and Prasanna, V. Graphsaint: Graph sampling based inductive learning method. *arXiv preprint arXiv:1907.04931*, 2019.

Zhang, J., Zhang, H., Xia, C., and Sun, L. Graph-bert: Only attention is needed for learning graph representations. *arXiv preprint arXiv:2001.05140*, 2020.

Zhao, J., Li, C., Wen, Q., Wang, Y., Liu, Y., Sun, H., Xie, X., and Ye, Y. Gophormer: Ego-graph transformer for node classification. *arXiv preprint arXiv:2110.13094*, 2021.

Zhu, C., Ping, W., Xiao, C., Shoeybi, M., Goldstein, T., Anandkumar, A., and Catanzaro, B. Long-short transformer: Efficient transformers for language and vision. *Advances in Neural Information Processing Systems*, 34, 2021.

Zhu, J., Yan, Y., Zhao, L., Heimann, M., Akoglu, L., and Koutra, D. Beyond homophily in graph neural networks: Current limitations and effective designs. *Advances in Neural Information Processing Systems*, 33:7793–7804, 2020.

A. More Theoretical Analysis

Note that in the demonstration process below, we assume positional information is already fused into node features.

Proposition A.1. *There exists a distribution of random projection matrices $P \in \mathbb{R}^{n\times k}$ such that for any linear weight matrices $W_K, W_Q, W_V \in \mathbb{R}^{f\times d}$, node feature matrix $X \in \mathbb{R}^{n\times f}$, mini-batch of nodes $X_B \in \mathbb{R}^{b\times f}$, column vector $v \in \mathbb{R}^n$ of XW_V, and any choice of $\varepsilon > 0$,*

$$\Pr\left(\|A_B PP^\top v - A_B v\|_F < \varepsilon \|A_B v\|_F\right) > 1 - O(1/n), \tag{10}$$

with $A_B = \mathrm{Softmax}\left(X_B W_Q \left(XW_K\right)^\top / \sqrt{d}\right)$ and $k = O\left(\log(n)/\varepsilon^2\right)$.

Our goal here is to find a projection matrix P to project both the attention matrix A_B and features v into some low dimension space, enabling us to replace the attention matrix $A_B \in \mathbb{R}^{b\times n}$ with $\widetilde{A}_B = A_B P \in \mathbb{R}^{b\times k}$ and $v \in \mathbb{R}^n$ with $\widetilde{v} = P^T v \in \mathbb{R}^k$. Despite the existence of such P matrix, we argue that it is impractical to apply Proposition A.1 in practice. The reason is that it is hard to materialize $\widetilde{A}_B$ in memory so the explicit computation of A_B is inevitable, which does not help improve scalability as calculating all attention matrices batch-by-batch is still $O(n^2)$. Below, we describe a route to escape this problem.

B. More Ablation Studies

Local range. To show the efficacy of our local module, we further run the ablation study to have nodes attend to 1-, 2-, 3-hop neighborhoods within the local transformer of GOAT. Results are included in Table 5. We can see that the local module plays an important role in extracting features from local fields and contributes to the final predictions of the GOAT model. Note that arxiv-year and snap-patents have 50% training samples.

Table 5: Ablation study on the hop range of GOAT local module.

	ogbn-arxiv	**arxiv-year (50%)**	**ogbn-products**	**snap-patents (50%)**
GOAT-local-1-hop	71.23	50.18	78.18	47.47
GOAT-local-2-hop	72.26	52.06	78.74	49.44
GOAT-local-3-hop	**72.41**	**53.57**	**82.00**	**54.97**

C. Proofs

This section lists theoretical proofs of our propositions and theorems.

C.1. Proof of Proposition A.1

Proof. To help build the proof, we utilize the Johnson–Lindenstrauss (JL) Lemma from Johnson & Lindenstrauss (1984); Kane & Nelson (2014).

Lemma C.1. *For any integer $d > 0$, and any $0 < \varepsilon, \delta < 1/2$, there exists a probability distribution on $k \times d$ real matrices for $k = \Theta(\varepsilon^{-2}\log(1/\delta))$ such that for any $x \in \mathbb{R}^d$,*

$$\underset{P}{\mathbb{P}}\left((1-\varepsilon)\|x\|_2 \le \|Px\|_2 \le (1+\varepsilon)\|x\|_2\right) > 1 - \delta. \tag{11}$$

Using Lemma C.1 and Boole's inequality, for any $x, y \in \mathbb{R}^{1\times n}$, we have

$$\Pr(\|xPP^\top y^\top - xy^\top\|_F \le \varepsilon\|xy^\top\|_F) > 1 - 2\delta.$$

Now we choose to swap x with any row vector a out of A_B and y with v so we have

$$\Pr(\|aPP^\top v^\top - av^\top\|_F \le \varepsilon\|av^\top\|_F) > 1 - 2\delta.$$

Leveraging Boole's inequality, we get

$$\Pr(\|A_B PP^\top v^\top - A_B v^\top\|_F \le \varepsilon \|A_B v^\top\|_F) > 1 - 2b\delta > 1 - 2n\delta.$$

By choosing δ to be $O(1/n^2)$ we finally get

$$\Pr(\|A_B PP^\top v^\top - A_B v^\top\|_F \le \varepsilon \|A_B v^\top\|_F) > 1 - O(1/n),$$

with $k = O\left(\log(n)/\varepsilon^2\right)$.

□

C.2. Proof of Theorem 3.2

Proof. We follow the techniques in Wang et al. (2020) to provide the proof. We define $P_A = \delta P$ and $P_V = e^{-\delta}P$, δ is a constant. We aim to prove

$$\Pr\left(\left\|\exp\left(SP\right)P^\top X_V - \exp(S)X_V\right\|_F \le \varepsilon \|\exp(S)\|_F \left\|X_V\right\|_F\right) > 1 - O(1/n), \tag{12}$$

where $X_V = XW_V$ for simplicity. Using triangle inequality, we have

$$\begin{aligned}\left\|\exp\left(SP\right)P^\top X_V - \exp(S)X_V\right\|_F \le \underbrace{\left\|\exp(S)PP^\top X_V - \exp(S)X_V\right\|_F}_{a} \\ + \underbrace{\left\|\exp\left(SP\right)P^\top X_V - \exp(S)PP^\top X_V\right\|_F}_{b}.\end{aligned}$$

For part a, based on Proposition 1, we have

$$a \le \varepsilon \|\exp(S)\|_F \left\|X_V\right\|_F.$$

For part b, we have

$$b \le \left\|\exp\left(SP\right) - \exp(S)P\right\|_F \|P^\top X_V\|_F.$$

Given that the exponential function is Lipschitz continuous in a compact region, and also based on the Equation C.1, we have

$$b \le o(\|\exp(S)\|_F \|X_V\|_F).$$

Based on part a and part b, we finally attain

$$\Pr\left(\left\|\exp\left(SP\right)P^\top X_V - \exp(S)X_V\right\|_F \le \varepsilon \|\exp(S)\|_F \left\|X_V\right\|_F\right) > 1 - O(1/n).$$

□

C.3. Proof of Theorem 3.3

Proof. This proof is built upon the usage of Lipschitz constant and quantization error.

$$\begin{aligned}\left\|\widetilde{X}_B^{\text{out}} - X_B^{\text{out}}\right\|_F &= \|\widetilde{A}_B\widetilde{X}W_V - A_B X W_V\|_F \\ &= \|f_W(\widetilde{X})\widetilde{X}W_V - f_W(X)XW_V\|_F \\ &\le \underbrace{\|f_W(\widetilde{X})\widetilde{X} - f_W(X)X\|_F}_{a}\|W_V\|_F,\end{aligned}$$

where for the part a, we have

$$\begin{aligned}a &= \|f_W(\widetilde{X})\widetilde{X} - f_W(X)\widetilde{X} + f_W(X)\widetilde{X} - f_W(X)X\|_F \\ &\le \|f_W(\widetilde{X}) - f_W(X)\|_F\|\widetilde{X}\|_F + \|f_W(X)\|_F\|\widetilde{X} - X\|_F.\end{aligned}$$

Note that

$$\|\widetilde{X}\|_F \le \|P\text{diag}^{-1}(\mathbf{1}_n P)P^\top\|_F\|X\|_F \le \sqrt{k}\|X\|_F,$$

$$\|X - \widetilde{X}\|_F \le \varepsilon\|X\|_F,$$

$$\|f_W(\widetilde{X}) - f_W(X)\|_F \le \text{lip}\,(f_W)\,\|X - \widetilde{X}\|_F.$$

When we assume $\|X\|_F = O(\|A_B\|_F)$, we have

$$\left\|\widetilde{X}_B^{\text{out}} - X_B^{\text{out}}\right\|_F \le \varepsilon \cdot [1 + O\,(\text{lip}\,(f_W))]\,\|A_B\|_F \cdot \|X\|_F \cdot \|W_V\|_F\,.$$

□

C.4. Proof of Corollary 3.4

Proof.

$$\widetilde{X}_B^{\text{out}} = \text{Softmax}\left(X_B W_Q(\widetilde{X}W_K)^\top/\sqrt{d}\right)\widetilde{X}W_V,$$

$$\widetilde{X}_B^{\text{out}} = \text{Softmax}\left(X_B W_Q\left(P\,\text{diag}^{-1}(\mathbf{1}_n P)\,P^\top X W_K\right)^\top/\sqrt{d}\right)P\,\text{diag}^{-1}(\mathbf{1}_n P)\,P^\top X W_V,$$

$$\widetilde{X}_B^{\text{out}} = \text{Softmax}\left(X_B W_Q\left(P\widetilde{K}\right)^\top/\sqrt{d}\right)P\widetilde{V},$$

$$\widetilde{X}_B^{\text{out}} = \text{Softmax}\left(X_B W_Q\widetilde{K}^\top P^\top/\sqrt{d}\right)P\widetilde{V},$$

note that the row vector of $P \in \mathbb{R}^{n\times k}$ is one-hot, so $X_B W_Q\widetilde{K}$ times $P^\top$ works as copying the attention scores according to the assignment of centroid of each node. In the same way, $\text{Softmax}(\cdot)P$ aggregates the Softmax logits based on the assignment through summation.

Say a random row vector x from X_B, $xW_Q\widetilde{K}^\top/\sqrt{d}$ is denoted as a row vector $[s_1, s_2, \ldots, s_k] \in \mathbb{R}^{1\times k}$, $(\mathbf{1}_n P)$ is denoted as $[n_1, n_2, \ldots, n_k]$, then we can see that

$$\left(\text{Softmax}\left(xW_Q\widetilde{K}^\top P^\top/\sqrt{d}\right)P\right)[i] = \frac{n_i\exp(s_i)}{\sum_{j=1}^k n_j\exp(s_j)},$$

so we can cancel the P both inside and outside Softmax by adding a weighting term to make the exponential computation weighted with the centroid size, where we attain

$$\widetilde{X}_B^{\text{out}} = \text{Softmax}\left(X_B W_Q \widetilde{K}^\top / \sqrt{d} + \log\left(\mathbf{1}_n P\right)\right) \widetilde{V}.$$

$\square$

D. Experimental Details

This section describes in more detail the experimental setup for the empirical results presented in Section 4.

D.1. Dataset Downloading

We refer readers to Hu et al. (2020a) and Lim et al. (2021) and their official repos for dataset downloading.

D.2. GOAT

For the hyperparameter selections of our GOAT model, besides what we have covered in the setup part of the experiment section that datasets share in common, we list other settings in Table 6. Each experiment is repeated four times to get the mean value and error bar. We use Adam optimizer with lr 1e-3.

Table 6: Proposed Model Dataset-Specific Hyperparameter Settings

Model	Dataset	# Heads	# Hidden Channels
GOAT	`ogbn-arxiv`	4	128
	`ogbn-products`	2	256
	`arxiv-year`	4	128
	`snap-patents`	2	128

D.3. Baseline Models

Since the heterophilius datasets on which we benchmark the GOAT model are derived from Lim et al. (2021), in order to facilitate as fair a comparison as possible, especially against the LINKX model proposed in the same work, we utilize their implementation provided at the official repo[1]. This library also provides reference implementations of other GNN architectures, and we utilize those as well. Following the procedure described both in the paper and implicitly by their codebase, we run a hyperaparameter sweep for each model on each dataset. For each combination of parameters, 5 models are trained using different initialization seeds to determine a mean value and error bars, and then the final hyperparameters are selected based on accuracy on the validation set. These final parameters correspond to the settings used to realize the "official train split" numbers in Table 2 in the main work for `ogbn-arxiv` and `ogbn-products` and the 50% train split numbers for `arxiv-year` and `snap-patents`. These same parameters are also used when performing the sample complexity experiments with train splits of 10% and 20% for the latter two datasets.

For the baseline GNNs we chose a Graph Convolutional Network with Jumping Knowledge (GCNJK) and a Graph Attention Network (GAT), and for a second heterophily-specific model to complement LINKX, we consider MixHop. As described in Section 4 of the main work, we use ERM to train all models including the baselines. We also focus on the minibatch setting rather than "full-batch" training as a primary feature of the GOAT model is its native scalability through minibatch training. The batching algorithm we use for the GCNJK, GAT, and MixHop models is the GraphSAINT Random Walk based sampler (LINKX uses its own adjacency row-wise sampling scheme, see Lim et al. (2021) for details). In the spirit of fair evaluation, we make the model and sampler choices based on the fact that according to Lim et al. (2021), each of these are the most performant two models in the homophily and heterophily-specific design categories on the datasets under evaluation.

Hyperparameter Settings: For all four baseline models we tune two main parameters: the number of layers, and the

[1]https://github.com/CUAI/Non-Homophily-Large-Scale

Table 7: Baseline Model Dataset-Specific Hyperparameter Settings

Model	Dataset	# Layers	# Hidden Channels	SAINT Batch Size
GAT	`ogbn-arxiv`	2	32	10,000
	`ogbn-products` *	–	–	–
	`arxiv-year`	2	32	10,000
	`snap-patents`	2	32	10,000
GCNJK	`ogbn-arxiv`	2	128	10,000
	`ogbn-products`	4	256	5,000
	`arxiv-year`	4	256	10,000
	`snap-patents`	2	256	10,000
MixHop	`ogbn-arxiv`	2	128	10,000
	`ogbn-products`	3	128	5,000
	`arxiv-year`	4	128	10,000
	`snap-patents`	2	128	10,000
LINKX	`ogbn-arxiv`	1	64	N/A
	`ogbn-products`	1	128	
	`arxiv-year`	1	256	
	`snap-patents`	1	16	

number of hidden channels (dimension) of each layer. We also evaluate two subgraph sizes, or batch sizes, for the SAINT sampler (number of roots used for the random walk). For the GAT model only, we also tune the number of attention heads. We evaluate the same parameter ranges described in Lim et al. (2021) and defined by their codebase, and simply report the final parameters selected in Table 7. Selected parameters that are shared amongst all model and dataset pairs include training for 500 epochs, using the AdamW optimizer with a learning rate of 0.01, and creating 5 SAINT subgraphs per epoch. Model specific selected parameters include using 8 heads for the GAT, concatenative jumping knowledge for the GCNJK model, and the 2 hop setting for MixHop. For all settings that we choose as final, if possible, we verify that the accuracy is within $\pm 1\%$ of the value reported in Lim et al. (2021) as "best" for each model on each dataset.

There are two details of particular note concerning Table 7 (and corresponding results in Table 2 in the main work). First, for the `snap-patents` dataset we do not use the ClusterGCN sampler for the MixHop architecture as it proved too time and memory intensive for our hardware. We ground this choice in the fact that according to the performance reported in Lim et al. (2021), the performance of MixHop with cluster sampling would still have been below the performance of GOAT by approximately 8 accuracy points. As an additional comment, the computational costliness of this method was also a challenge in their work, precluding it from parts of their evaluation. In the spirit of scalability, overall, we see GraphSAINT as being a more relevant choice for our comparison due to its more favorable scaling characteristics.

Second, also in service of a competitive evaluation, we chose to report performance of the GAT model on `ogbn-products` * pulled from the Open Graph Benchmark's official leaderboard[2] for this dataset since the mini-batch performance we achieved with the SAINT sampler was significantly lower than the reference result (as well as that of our GOAT model). The result from the leaderboard was trained using the neighbor sampling algorithm.

For Fig 4a and Fig 4b, we set batch size as 10K. We use 4K as codebook size. GAT leverages NS [20,10,5] to do minibatching. The total running time involve evaluation time.

[2]https://ogb.stanford.edu/docs/leader_nodeprop/